MODELLING INTERANNUAL VARIATIONS OF SUMMER MONSOONS

T.N.Palmer, C.Brankovic, P.Viterbo and M.J.Miller
European Centre for Medium Range Weather Forecasts
Reading,UK

ABSTRACT

Results from a set of 90-day integrations, made with a T42 version of the ECMWF model, and forced with a variety of specified sea surface temperature (SST) datatsets, are discussed. Most of the integrations started from data for 1 June 1987 and 1 June 1988. During the summer of 1987, both the Indian and African monsoons were weak, in contrast with the summer of 1988 when both monsoons were much stronger. With observed SSTs, the model is able to simulate the interannual variations in the global scale velocity potential and streamfunction fields on seasonal timescales. On a regional basis, rainfall over the Sahel and, to a lesser extent, India showed the correct sense of interannual variation, though in absolute terms, the model appears to have an overall dry bias in these areas.

Additional integrations were made to study the impact of the observed SST anomalies in individual oceans. Much of the interannual variation in both Indian and African rainfall could be accounted for by the remote effect of the tropical Pacific SST anomalies only. By comparison with the effect of the Pacific, interannual variability in Indian Ocean, tropical Atlantic Ocean, or extratropical SSTs had little influence on tropical large-scale flow or rainfall in the areas studied.

Integrations run with identical SSTs, but different initial conditions indicated that for large-scale circulation diagnostics, the impact of anomalous ocean forcing dominated the possible impact of variations in initial conditions. In terms of local rainfall amounts, on the other hand, the impact of initial conditions is comparable with that of SST anomaly over parts of India and south east Asia, less so over the Sahel. This suggests that a non-negligible fraction of the variance of month to seasonal mean rainfall on the regional scale, may not be dynamically predictable.

1. INTRODUCTION

A major component of the Tropical Ocean/Global Atmosphere (TOGA) programme is focussed towards the development of a seasonal-timescale prediction capability using global coupled ocean-atmosphere general circulation models. In order to test the potential of such models for seasonal forecasting, it is necessary to assess how well they can simulate interannual variations in regional climate when the observed sea surface temperatures (SSTs) for a given season are prescribed (ie assuming a 'perfect' ocean model environment). Some aspects of this question have already been addressed by model intercomparison studies of the large-scale atmospheric response to (northern) wintertime El Nino SST anomalies (WMO, 1986, 1988). However, of particular practical importance in this respect are the interannual variations in summer monsoon rains, since failure of these rains almost invariably has devastating consequences on crop production for the countries affected.

In addition, such seasonal integrations are relevant to the needs of shorter timescale weather prediction. Long integrations of numerical weather prediction (NWP) models allows an assessment of systematic

biases in the simulation of atmospheric low-frequency variability. The ability to simulate the correct climatological frequency of blocking events, for example, is of paramount importance in medium-range NWP.

In this paper we present some results from a set of seasonal integrations made with the T42 version of the ECMWF NWP model over the northern summers of 1987 and 1988, with specified SST. These years were of particular interest for their contrasting behaviour in monsoon regions (Krishnamurti et al, 1989, 1990). In particular, 1987 was a severe drought year over both India and the African Sahel, whilst 1988 was an above average monsoon year for India, and rains over the Sahel were close to the climatological mean. During these two years, the El Nino/ Southern Oscillation (ENSO) cycle swung from warm to cold phase. We shall focus our discussion on the ability of the ECMWF model to simulate both global and regional seasonal and monthly mean monsoon circulations and associated rainfalls during the northern summer. Additional integrations designed to study the influence of SST anomalies in the individual oceans, and the sensitivity of month and seasonal mean fields to initial conditions, are also described.

2. EXPERIMENTAL DESIGN

All integrations considered here are 90 days in duration, and were intitialised from ECMWF operational archived data from 1 June 1987 or 1 June 1988 (except for one integration started on 2 June 1988). The integrations were made with a T42L19 version of the (CY34) ECMWF model (Simmons et al., 1988), but without cumulus momentum transports and including a revision to the bulk parametrization of sensible and latent heat flux. The principal effect of this revision, described in a companion paper (Miller et al., 1991) was to increase surface evaporation significantly in regions of weak gridbox mean wind. As shown in Miller et al., the new treatement of the fluxes had a substantial impact on the model's sensitivity to SST anomalies in the warm pool regions.

The integrations were made with a number of specified SST datatsets, updated from 5 day mean files. The experiments are summarised in Table 1.

In this study, climatological SSTs were taken from the Reynolds and Roberts (1987) dataset (see also Reynolds 1988). Observed SSTs were taken from the National Meteorological Center SST analyses used for operational ECMWF forecasts. Differences between the observed and climatological SST for the individual months of June, July and August of both years are shown in Fig.1. It can be seen that a number of features are common to both years, notably the relative warming in the equatorial and south Atlantic and Indian Oceans. In addition, the extratropical north Pacific is cooler. This pattern

INTEGRATION	INITIAL DATE	SST
87O	1/6/87	Observed
87C	1/6/87	Climatological
88O	1/6/88	Observed
88C	1/6/88	Climatological
88O*	2/6/88	Observed
87OP	1/6/87	Observed in tropical Pacific, climatological elsewhere
87OI	1/6/87	Observed in tropical Indian Ocean, climatological elsewhere
87OA	1/6/87	Observed in tropical Atlantic, climatological elsewhere
87OE	1/6/87	Observed in the extratropics, climatological elsewhere
88OP	1/6/88	Observed in tropical Pacific, climatological elsewhere
88OI	1/6/88	Observed in tropical Indian Ocean, climatological elsewhere
88OA	1/6/88	Observed in tropical Atlantic, climatological elsewhere
88OE	1/6/88	Observed in the extratropics, climatological elsewhere

TABLE 1

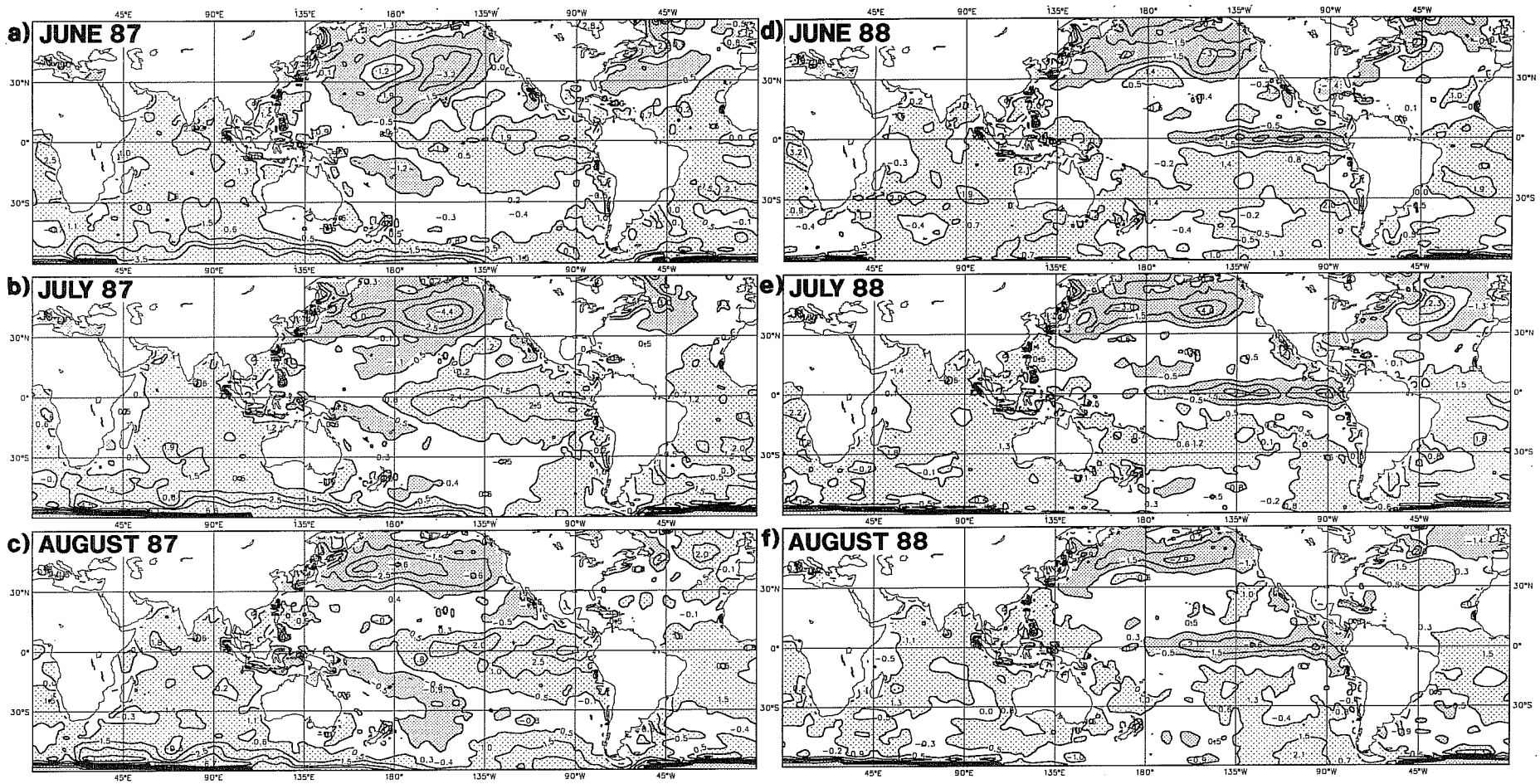

Fig. 1 Sea surface temperature anomalies for a) June 1987, b) July 1987, c) August 1987, d) June 1988, e) July 1988, f) August 1988. Contour interval 1K with ± 0.5K contoured. Coarse stipple >0.5K, fine stipple <-0.5K.

is fairly consistent with patterns of interdecadal variability over the last three decades studied from other analyses of SST (e.g. Folland et al., 1984, 1986).

In addition, however, these maps reveal clear evidence of interannual variability, primarily associated with ENSO, which swung from warm to cold phase between these two years, with SST anomalies in the equatorial eastern Pacific evolving from more than +2K in 1987 to more than -2K in 1988. Note that the cold pool in 1988 was restricted to a few degrees from the equator, whilst the warm pool in 1987 had much greater latitudinal extent. For reference, we show in Fig.2 the monthly mean differences between SST in 1988 and 1987. The effects of El Nino is dominant over the whole season in the tropical Pacific Ocean. There is a tendency for the Indian ocean SSTs to be cooler in 1988 than 1987 (up to 1K degree in June). This may be associated with the effect of the relatively strong atmospheric monsoon flow in 1988 on the ocean (Shukla, 1987).

For the 'individual ocean' experiments desribed in Table 1, the boundary between the Indian and Pacific Oceans was taken at 120E. Where SST anomalies were included in the 'tropics' only, they were taken from 30S to 30N. Where SST anomalies were included in the 'extratropics' only, they were taken poleward of 30 degrees.

3. GLOBAL DIAGNOSTICS

3.1 Integrations with global SST anomalies

For verification purposes we show in Fig.3 maps of seasonal mean (JJA) 200mb velocity potential (left hand column) and streamfunction anomalies (right hand column) for 1987 and 1988 from ECMWF analyses. The 'climate' used to construct these anomalies is a mean of ECMWF analyses over 5 summers from 1985 to 1989; analyses of tropical divergent flow, taken from years earlier than this, suffer from serious deficiencies and were therefore not included. The reference climate fields are shown in the bottom panels in Fig.3 (e and f).

Fig.3 shows clear evidence of significant large-scale atmospheric interannual variability. Over the eastern Pacific, consistent with the differences in SST, there is anomalous large-scale 200mb divergence in 1987 (Fig.3a) and anomalous convergence in 1988 (Fig.3c). In 1987, the anomalous divergence extends across the Atlantic, with anomalous convergence over Indonesia and south east Asia. In 1988, the anomalous Pacific convergence extends across the whole Pacific, with relatively strong anomalous divergence centred over the western Indian Ocean. The anomalous rotational wind is predominantly westerly across the tropics in 1987 (Fig.3b), and easterly, particularly over the Atlantic, in 1988 (Fig.3d).

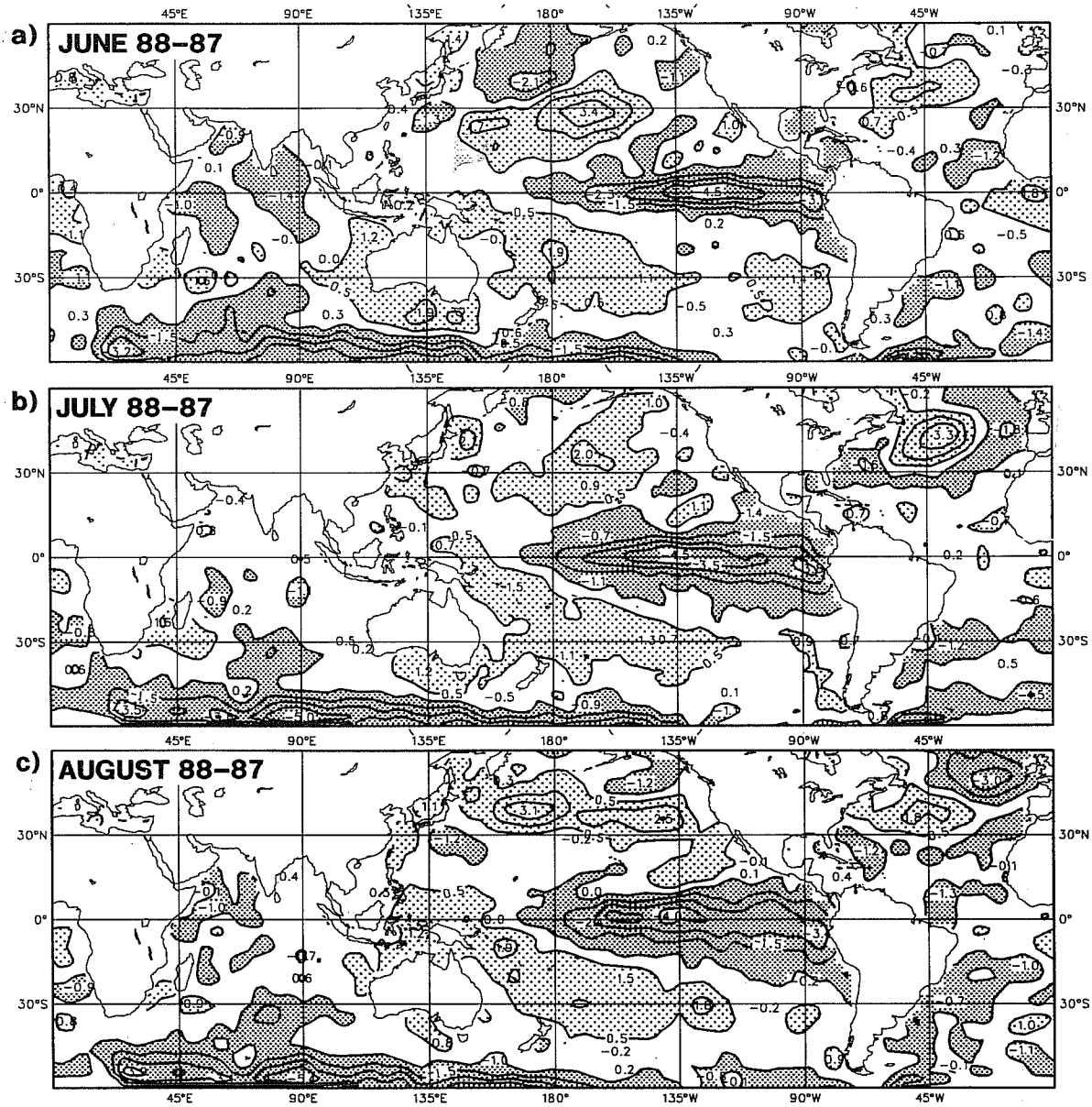

Fig. 2. Sea surface temperature differences between 1988 and 1987 for a) June, b) July, c) August. Contour interval 1K with ± 0.5K contoured. Coarse stipple >0.5K, fine stipple <-0.5K.

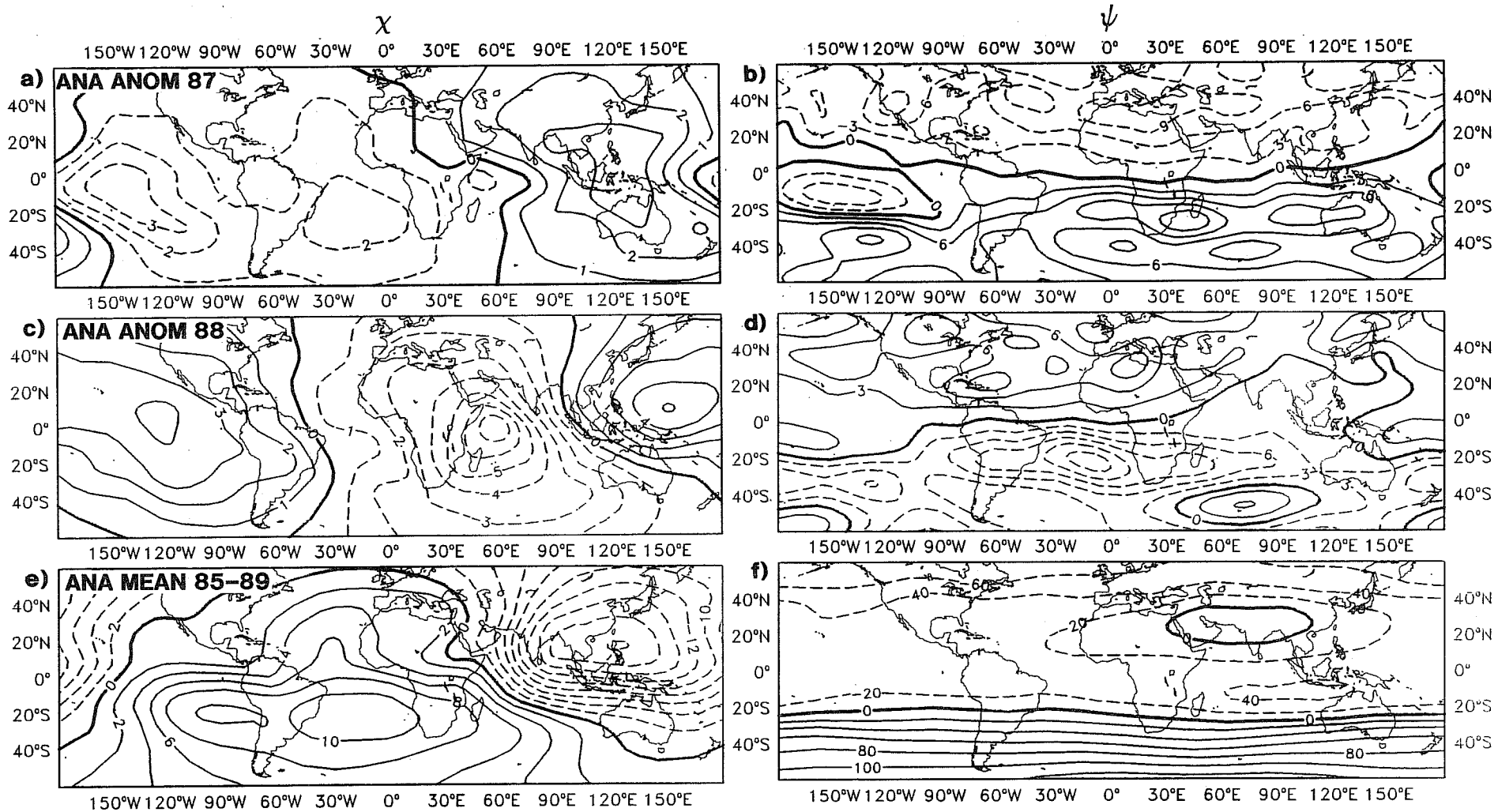

Fig. 3 a) JJA 200mb velocity potential anomaly. ECMWF analysis for 1987. Contour interval ($1x10^6m^2s^{-1}$). b) JJA 200mb streamfunction anomaly. ECMWF analysis for 1987. Contour interval ($3x10^6m^2s^{-1}$). c) as a) but for 1988. d) as b) but for 1988. e) climatological mean 200mb velocity potential. Contour interval ($2x10^6m^2s^{-1}$). f) climatological mean 200mb streamfunction anomaly. Contour interval ($20x10^6m^2s^{-1}$).

Fig.4 shows the 90-day mean 200mb velocity potential and streamfunction for the differences (87O-87C) and (88O-88C) between experiments with observed and climatological SSTs. For reference, we also show in the bottom panels in Fig.4 (e and f) the full fields averaged for 87C and 88C.

For 87O-87C, the simulated pattern of large-scale divergence (Fig.4a) corresponds reasonably to Fig.3a, with anomalous convergence over the Pacific and the Atlantic. However, the anomalous divergence is positioned further west than in Fig.3a. Moreover, the amplitude of the response is much larger than in Fig.3a. The pattern of 200mb streamfunction for 87O-87C (Fig.4b), broadly in agreement with the observed anomalies. In particular, in both model and analysis (Fig.3b), there are strong westerly anomalies over much of the tropics during 1987, excluding the eastern Pacific, though again, the model response is stronger in amplitude.

For 88O-88C, both the amplitude and the simulated pattern of large-scale divergence (Fig.4c) is broadly similar to that analysed, though there is a less pronounced minimum over the western Indian Ocean than in Fig.3a. The streamfunction difference for 88O-88C (Fig.4d) correctly shows anomalous westerlies over the equatorial Pacifc, and anomalous easterlies over south America and the tropical Atlantic.

The full field streamfunction (Fig.4f) compares well with the analysed climatological full field (Fig.3f), and both maps show clearly the upper level Tibetan high, associated with the Asian monsoon flow. The full field velocity potential in model and analysis (Fig.4e and 3e) similarly compares well over Asia, though the model appears to have developed erroneous divergence over central America.

Quantitative comparison of Figs 3 and 4 is not stricly possible because of ambiguities in the calculation of atmospheric and SST climatologies. Hence, in order to verify the integrations 87O and 88O in a way that is independent of climate, we show in Fig.5a,b the analysed differences in 200mb velocity potential and streamfunction between JJA 1988 and 1987, and in Fig.5 c,d the difference in these fields between 88O and 87O. It can be seen that whilst the overall simulated pattern is quite realistic, the model response, particularly in terms of the velocity potential, is again somewhat strong. On the basis of these results, it is possible that the model is too responsive to the warm El Nino SST anomalies of 1987; on the other hand, the analyses themselves were made with versions of the ECMWF model which predate the one used for the integrations here (in particular not including the flux revision described in Miller et al., 1991), introducing further uncertainty in the verification process.

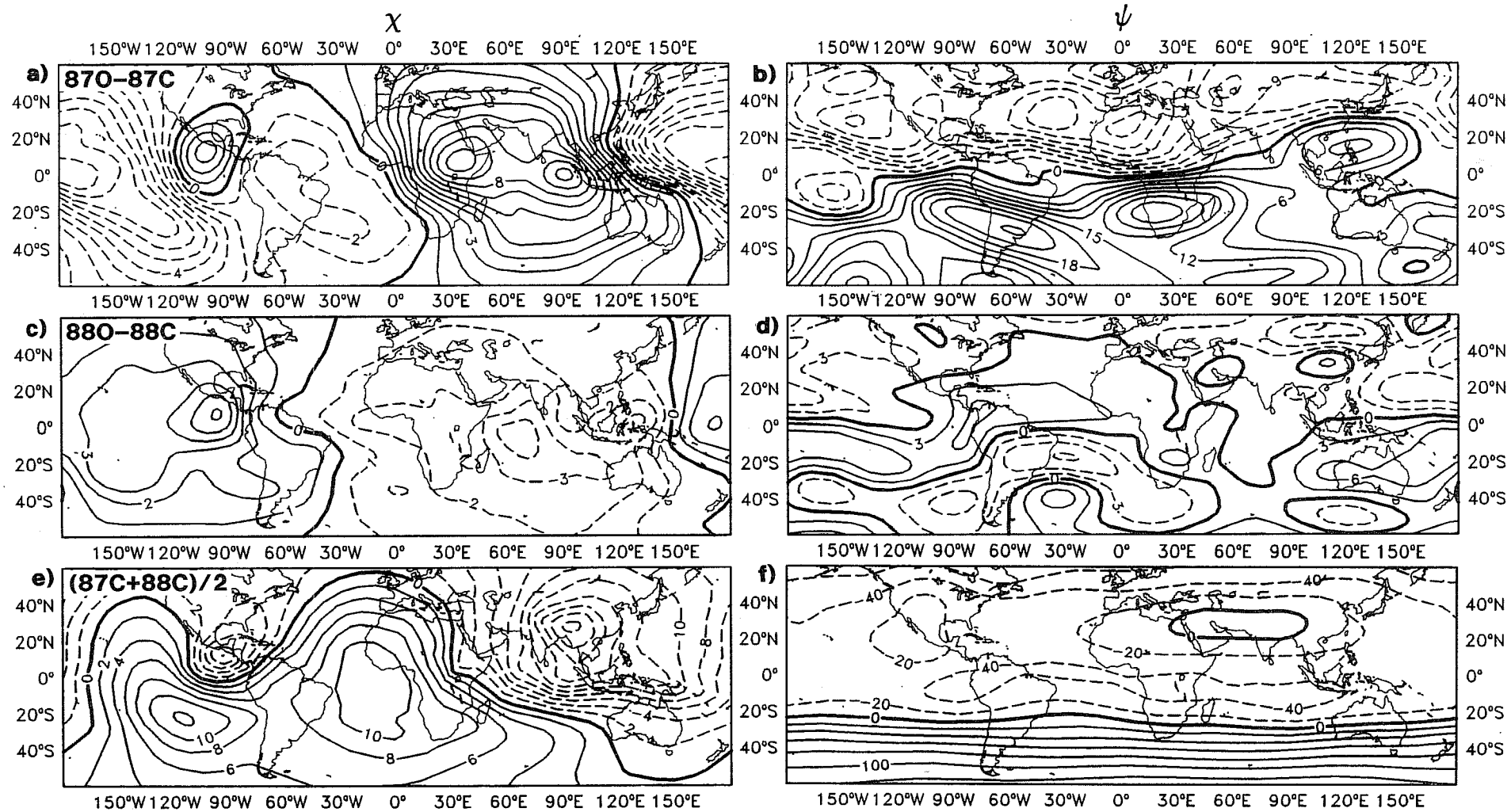

Fig. 4 a) 87O-87C days 1-90 200mb velocity potential. Contour interval ($1x10^6 m^2 s^{-1}$) b) 87O-87C days 1-90 200mb streamfunction. Contour interval ($3x10^6 m^2 s^{-1}$). c) as a) for 88O-88C. d) as b) for 88O-88C. e) (87C+88C)/2 days 1-90 200mb velocity potential. Contour interval ($2x10^6 m^2 s^{-1}$). f) (87C+88C)/2 days 1-90 200mb streamfunction. Contour interval ($20x10^6 m^2 s^{-1}$).

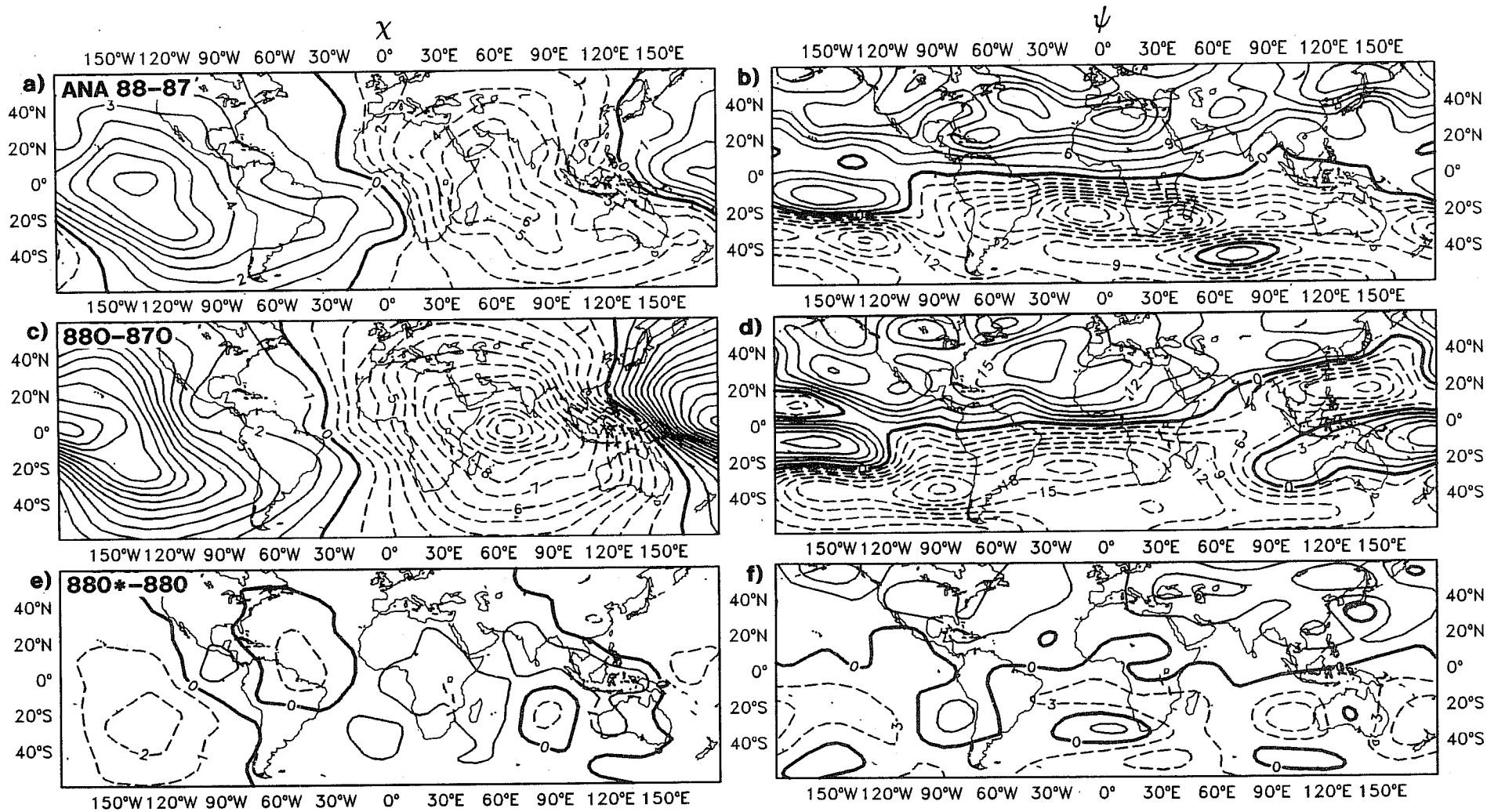

Fig. 5 a) ECMWF analysis difference 1988-1987 JJA 200mb velocity potential, b) ECMWF analysis difference 1988-1987 JJA 200mb streamfunction c) 88O-87O days 1-90 velocity potential. d) 88O-87O days 1-90 200mb streamfunction. e) as c) for 88O*-88O. f) as d) for 88O*-88O. a),c),e) contour interval ($1x10^6 m^2 s^{-1}$) b),d),f) contour interval ($3x10^6 m^2 s^{-1}$).

It is clear that studies such as these would benefit from consistent SST and atmospheric climatological datasets, and lend support to the requirement for atmospheric reanalysis (Bengtsson and Shukla, 1988).

3.2 Impact of initial conditions

As emphasised by Charney and Shukla (1981), seasonal predictability of the monsoons arises in part because the evolution of the large-scale tropical atmosphere is relatively insensitive to atmospheric initial conditions, in comparison with its dependence on boundary conditions, SST in particular. This can be seen in Fig.5e,f which show the difference (88O*-88O) in 90-day mean 200mb velocity potential and streamfunction; integrations with identical SST but initial conditions one day apart. Compared with the differences shown in Fig.5 c,d, it can be seen, particularly in the tropics, that the response to different SST overwhelms the response in the large-scale flow to differences in initial conditions.

As a further test of the sensitivity of the tropical forecasts to initial conditions, velocity potential and streamfunction differences between integrations 88C and 87C, initialised one year apart and run with identical SSTs, have been calculated (but are not shown). Again, the response is very small compared to that shown in Fig.5a-d.

Despite the relative insensitivity of these global diagnostics to initial conditions, it will be shown in section 4c that over parts of the Indian Ocean, SE Asia, and the Western Pacific, regional values of monthly-mean rainfall differences are sensitive to the initial conditions.

3.3 Integrations with regional SST anomalies

To explore further whether the global response to the full SST anomalies, as shown in Figs 4 and 5, can be understood in terms of the the sum of the responses to the individual oceans, Figs 6 and 7 show 90-day mean 200mb velocity potential and streamfunction anomalies for the individual ocean experiments.

With tropical Pacific SST anomalies only, Fig.6a (87OP-87C) shows a large-scale response in velocity potential very similar indeed to the full response in Fig.4a. The amplitude of this pattern is even larger than with the global SST anomalies. With tropical Indian ocean anomalies only, Fig.6c, (87OI-87C) shows a more localised response, predominantly comprising anomalous divergence over the Indian Ocean. The effect of the tropical Atlantic Ocean SST anomalies, Fig.6e (87OA-87C) is felt mainly over the Atlantic (anomalous divergence) and the eastern Pacific (anomalous convergence). Finally, Fig.6g shows the velocity potential response (87OE-87C) to the extratropical SST anomalies. It can

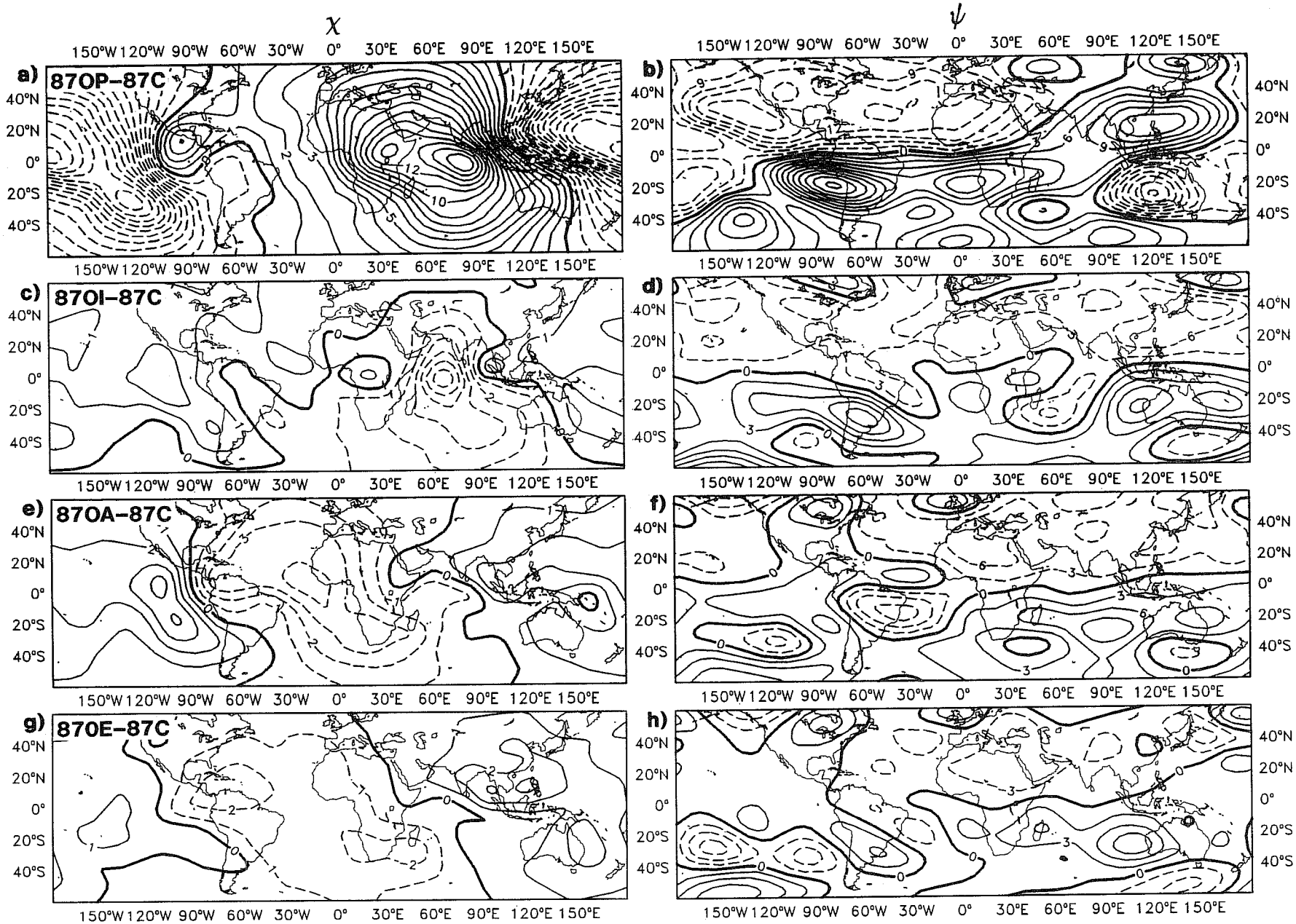

Fig. 6 a) 87OP-87C days 1-90 200mb velocity potential. Contour interval ($1x10^6 m^2 s^{-1}$) b) 87OP-87C days 1-90 200mb streamfunction. Contour interval ($3x10^6 m^2 s^{-1}$). c) as a) for 87OI-87C. d) as b) for 87OI-87C. e) as a) for 87OA-87C. f) as b) for 87OA-87C. g) as a) for 87OE-87C. h) as b) for 87OE-87C.

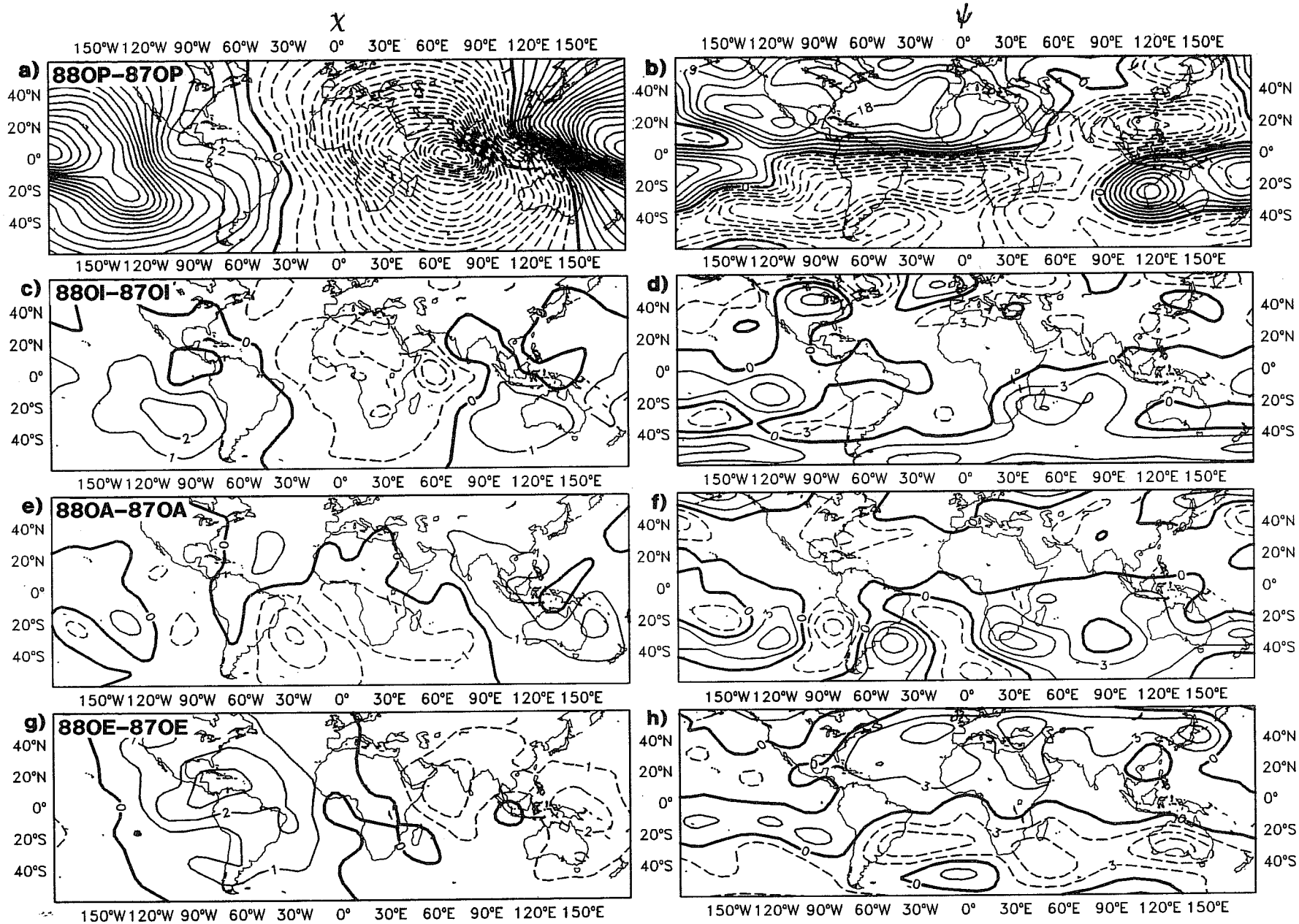

Fig. 7 a) 88OP-87OP days 1-90 200mb velocity potential. Contour interval ($1x10^6 m^2 s^{-1}$) b) 88OP-87OP days 1-90 200mb streamfunction. Contour interval ($3x10^6 m^2 s^{-1}$). c) as a) for 88OI-87OI. d) as b) for 88OI-87OI. e) as a) for 88OA-87OA. f) as b) for 88OA-87OA. g) as a) for 88OE-87OE. h) as b) for 88OE-87OE.

be seen that, compared with any of the tropical SST anomalies, the response in the tropics to extratropical SST anomalies is weak.

The streamfunction response to the 1987 tropical Pacific anomalies is shown in Fig.6b. Between the two centres of anomalous velocity potential over the Pacific and Indian Ocean are anomalous equatorial easterlies, with strong anticyclonic anomalies in both hemispheres at about 120E. To the east, over the tropical South America, the Atlantic and Africa, are anomalous westerlies. This overall pattern qualitatively resembles Gill's (1980) linear model response to imposed tropical heating anomalies. The equatorial streamfunction response both to the Indian Ocean (Fig.6d), and Atlantic Ocean (Fig.6f) SST anomalies for 1987 comprises relatively weak anomalous westerlies over the West Pacific, and anomalous easterlies over the Atlantic, respectively. The effect of the extratropical SST anomalies on the tropical streamfunction field is again relatively weak (Fig.6h).

It can be seen from Fig.6 that in terms of these large-scale atmospheric flow diagnostics, the linear sum of the individual ocean experiments approximately resembles the response to the global ocean anomalies (Fig.4a,b). In this respect, for (87O-87C), the effects of the Indian Ocean and the Pacific SST anomalies are partially cancelling over the Indian Ocean. Similarly the Atlantic SST anomalies tend to partially cancel the effect of the Pacific anomalies over the Pacific itself.

The upper air results for 1988 are consistent with those for 1987 (but not shown, for reasons of space). The response in velocity potential and streamfunction to the Pacific SST anomalies in the La Nina year 1988 (88OP-88C) is broadly opposite to the response for 1987 shown in Fig.6a,e, though the magnitude of the response is weaker in 88OP. The difference in the magnitude of the response is possibly associated with the fact that the spatial extent of the cold pool was much smaller in the summer of 1988, than the spatial extent of the warm pool in 1987 (cf Fig.1). As noted above, the 1988 SST anomalies in the tropical Atlantic and Indian Oceans are aproximately the same as for 1987. Consistent with this, the patterns of difference fields (88OI-88C) and (88OA-88C) are approximately the same as (87OI-87C) and (87OA-87C) respectively, both in terms of velocity potential and streamfunction. The response to extratropical SST anomalies (88OE-88C) is again relatively small.

As discussed above, the difference between observed and climatological SSTs for the Indian and Atlantic Oceans in particular, may principally reflect interdecadal, rather than interannual variability. In order to study the impact of interannual variations in regional SST we show in Fig.7 the 200mb velocity potential and streamfunction differences between 88OP-87OP, 88OI-87OI and 88OE-87OE. The results clearly show the predominance of the remote effect of El Nino. By comparison the impact of the other ocean SST differences are quite negligible. Moreover, it is difficult to ascribe any

statistical significance to the non-Pacific response. For example, the velocity potential difference over the western Indian Ocean in Fig.7b (88OI-87OI) changes sign between the second and third months of the integrations. In particular, therefore, we would assert that the remote effect of El Nino is overwhelmingly more important in determining interannual variability of the Asian monsoon than the more local effect of Indian Ocean SST anomalies.

4. REGIONAL DIAGNOSTICS

4.1 Integrations with global SST anomalies

In this subsection we discuss regional simulation of rainfall and low-level flow for the simulations 87O and 88O, focussing on the African Sahel and Asian monsoons. Successful simulations of interdecadal fluctuations in rainfall over the Sahel, using the UK Meteorological Office model, have been presented by Folland et al. (1986, 1989). Palmer et al. (1990) found a relatively good agreement between observed and predicted interannual variation of monthly monsoon rainfall for the Sahel, though less good for the south Asian region.

4.1.1 The Sahel

Fig.8a,b shows the ECMWF analysed moisture flux for July/August for 1987 and 1988 for level 17 of the model (about 970mb). Values geater than 50 g/kg m/s are shown stippled. There are a number of characteristics of the moisture flux that are consistent with earlier studies of Lamb (1983). However, the most striking differences lie to the east of Lake Chad, where in 1988, relatively strong fluxes extend across the African continent, almost to the Red Sea. These differences are captured well by the model simulations (87O and 88O) as shown in Fig.8c,d. Note, for example, the relatively strong moisture flux across to Sudan in 88O.

Rainfall maps associated with the Intertropical Convergence Zone (ITCZ) over Africa for July and August in 87O and 88O are shown in Fig.9. The relative dryness in 87O is apparent for both months. In parts of the Sahel around 15N, there is essentially no July rainfall in 87O, whilst in 88O, values generally lie between 1 and 2 mm/day. In August of both years, the ITCZ has moved north, and rainfall values over the Sahel have increased. However, as for July, values are noticeably weaker in 1987 than in 1988, which have rates up to 4mm/ day. Note also the 'tongue' of rainfall over Ethiopia and the Red Sea in 88O, absent in 87O.

In order to verify these rainfall amounts, we show in Fig.10 monthly-mean station values in the Sahel from WMO CLIMAT reports (obtained from the United Kingdom Meteorological Office) for July

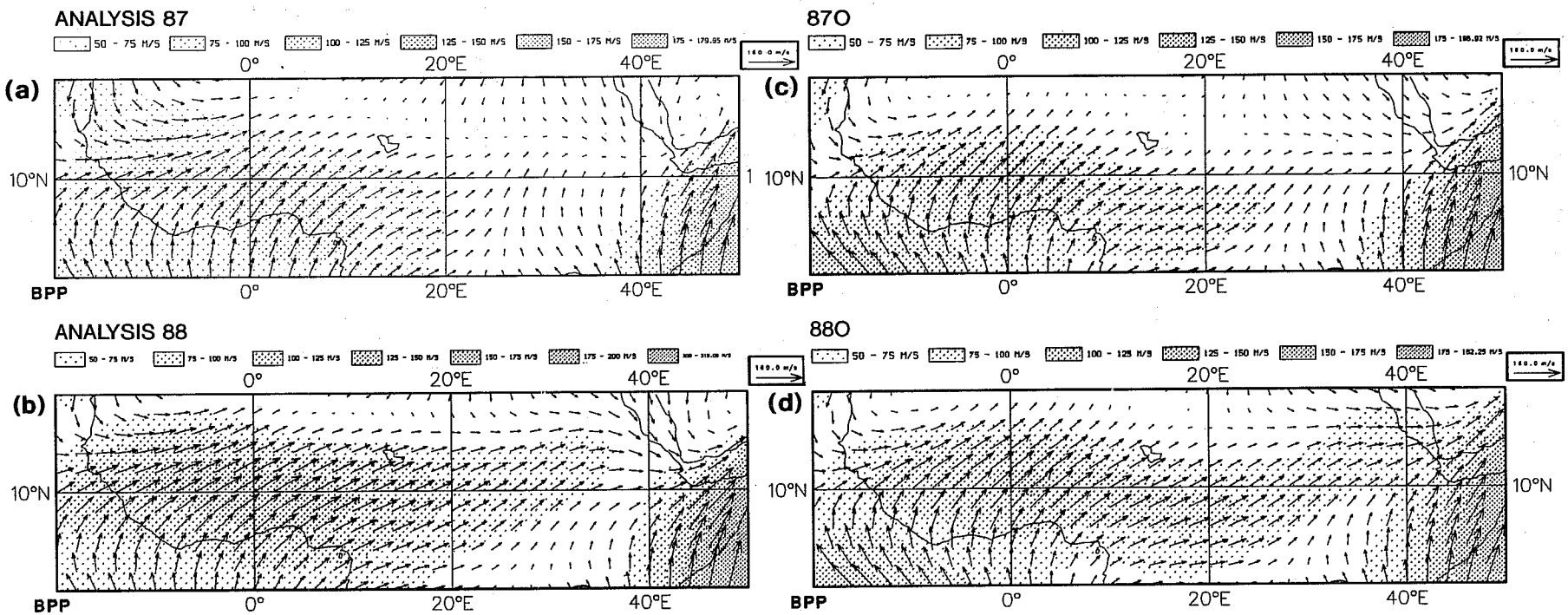

Fig. 8 Level 17 moisture flux (g/kg m/s; July/August mean) over the African Sahel. a) ECMWF analyses for 1987, b) ECMWF analyses for 1988, c) 87O, d) 88O. Stippled > 50g/kg m/s.

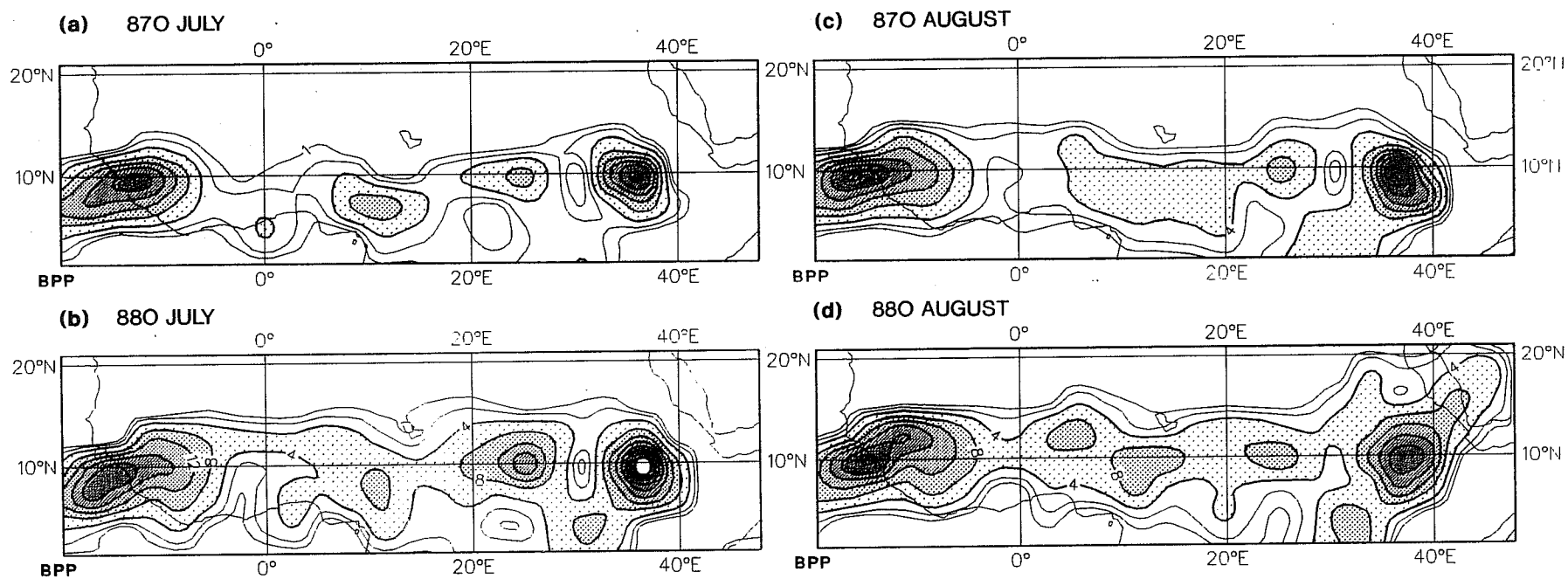

Fig. 9 Modelled rainfall over the African Sahel (mm/day). a) 87O July b) 88O July c) 87O August d) 88O August. Contours at 1,2,4,8,12,16... mm/day, stippled if greater than 4mm/day.

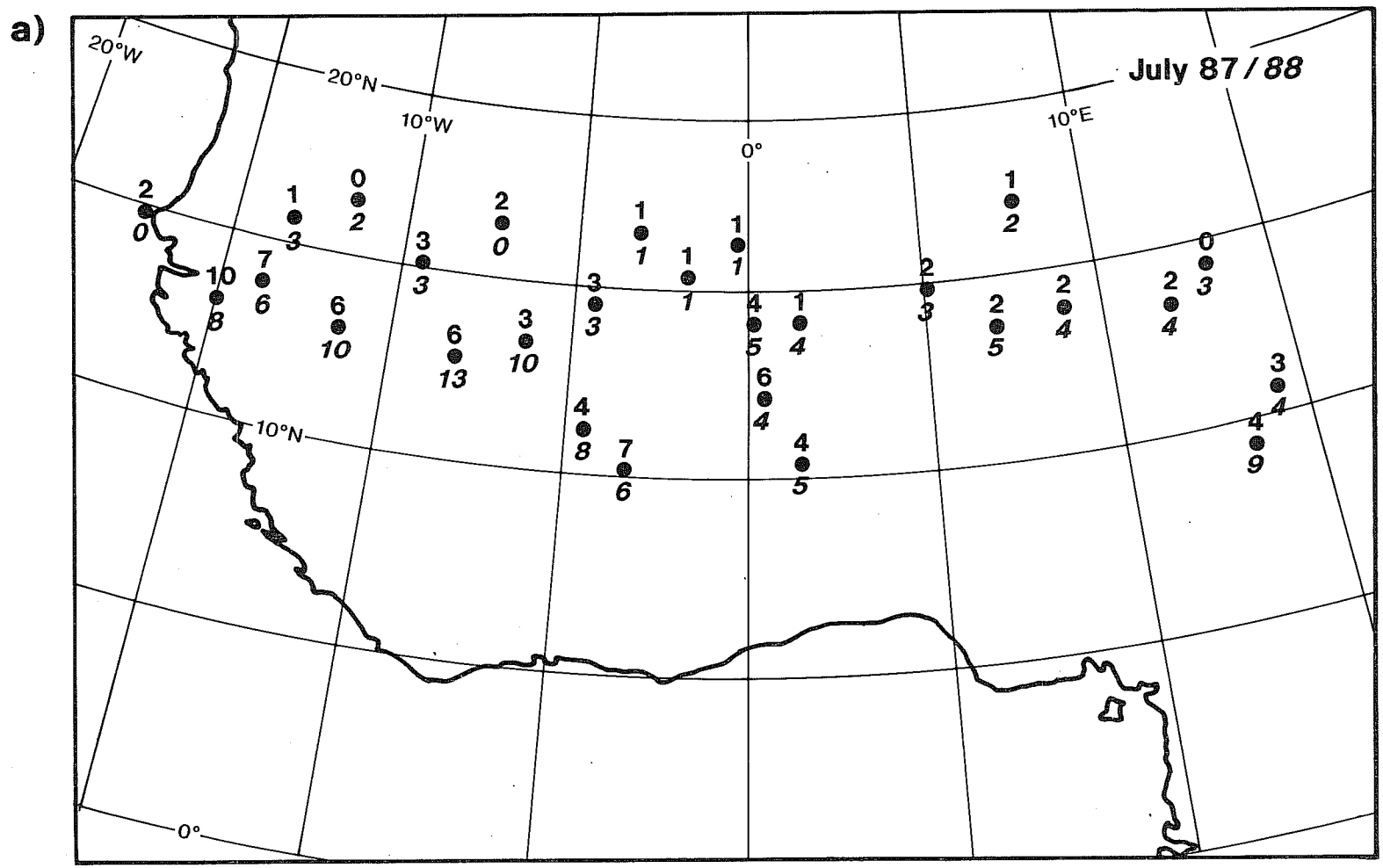

Fig. 10 Observed monthly mean station rainfall over African Sahel (mm/day) based on WMO CLIMAT data. Values above station dot are for 1987, values below station dot are for 1988. a) July 1987/1988 b) August 1987/1988.

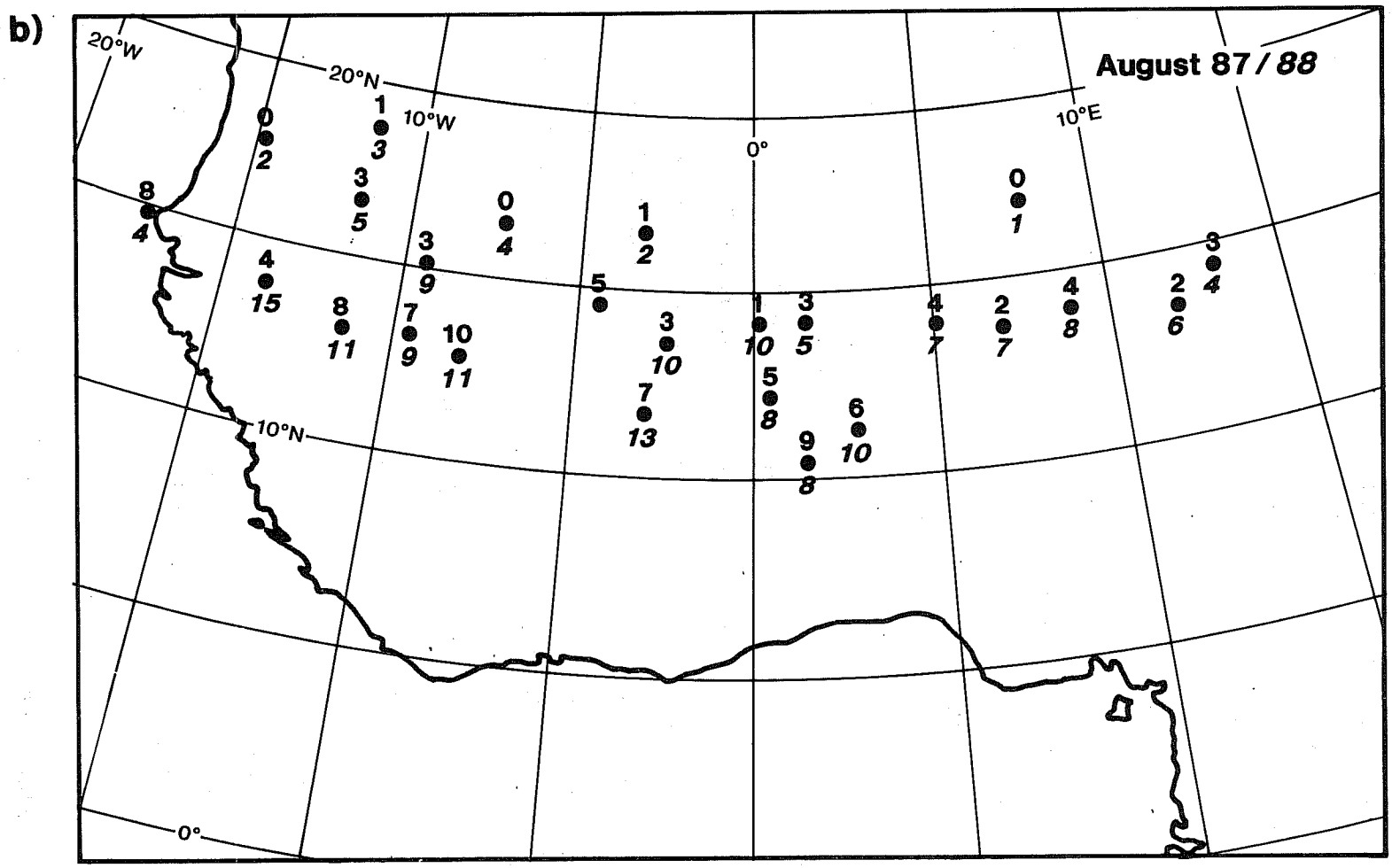

Fig.10 b)

and August 1987 (figures above station) and 1988 (figures below station). In July (Fig.10a), rainfall rates are generally higher in 1988 than in 1987 except perhaps for stations near the Atlantic coast. In the latitude band around 15N to the east of the Greenwich meridian, values lie around 2mm/day in 1987, and 4 mm/day in 1988. In August (Fig.10b), the difference between the relatively wet year in 1988 and the relatively dry year of 1987 can be clearly seen in most of the station values. At 15N values in 1988 are up to about 8mm/day, yet only about 3 mm/day in 1987. Whilst observed rainfall rates over Ethiopia and surrounding areas are not shown, the 'tongue' of relatively strong rain in Fig.9d does appear to be realistic. The flooding of the Nile during the summer of 1988 was well documented.

Compared with these station values, the model appears to have an overall dry bias. On the other hand the principal sense of interannual variation is captured by the model simulations. On this basis it is possible that the bias may reflect shortcomings in parametrizations of land surface hydrology, rather than any fundamental bias in processes affecting the large-scale general circulation of the model.

4.1.2 India

Analysed and simulated seasonal mean 850mb winds for 1987 and 1988, over the Indian Ocean are shown in Fig.11. The analysed low-level wind maximum off the Somali coast is a little stronger in 1988 (Fig.11a,b). On the other hand, over India, the Bay of Bengal and parts of SE Asia, the low-level flow is stronger in 1987. In the integrations 87O and 88O, there is clearly a systematic westerly bias in the winds of more than 5m/s in places. Nevertheless the analysed interannual differences over India, the Bay of Bengal, and SE Asia, have been captured, with noticeable stronger winds in 87O. On the other hand, the somewhat stronger analysed Somali wind maximum in 88O has not been simulated.

Fig.12 shows monthly mean rainfall maps from 87O and 88O for July and August. In 87O, much of the interior of India receives less than 1mm/day in July (Fig.12a). For 88O, in these areas, the comparable rates are up to 4mm/day (Fig.12b). The west coast maximum is also stronger in 88O than in 87O. These differences are consistent with the 90 day mean 200mb velocity potential maps discussed above. Fig.12c,d shows rainfall for August from 87O and 88O. Rainfall in the interior of India has increased from July values in both 87O and 88O, however, overall values for 87O are still noticeably weaker than in 88O. On the other hand, it is interesting to note that the rainfall maximum on the west coast is now somewhat weaker in 88O than in 87O.

Observed rainfall values over India are given in Fig.13 for July and August 1987 and 1988. These values are subdivisional monthly means as reported in Mausam (Das et al., 1988, 1989). The relative

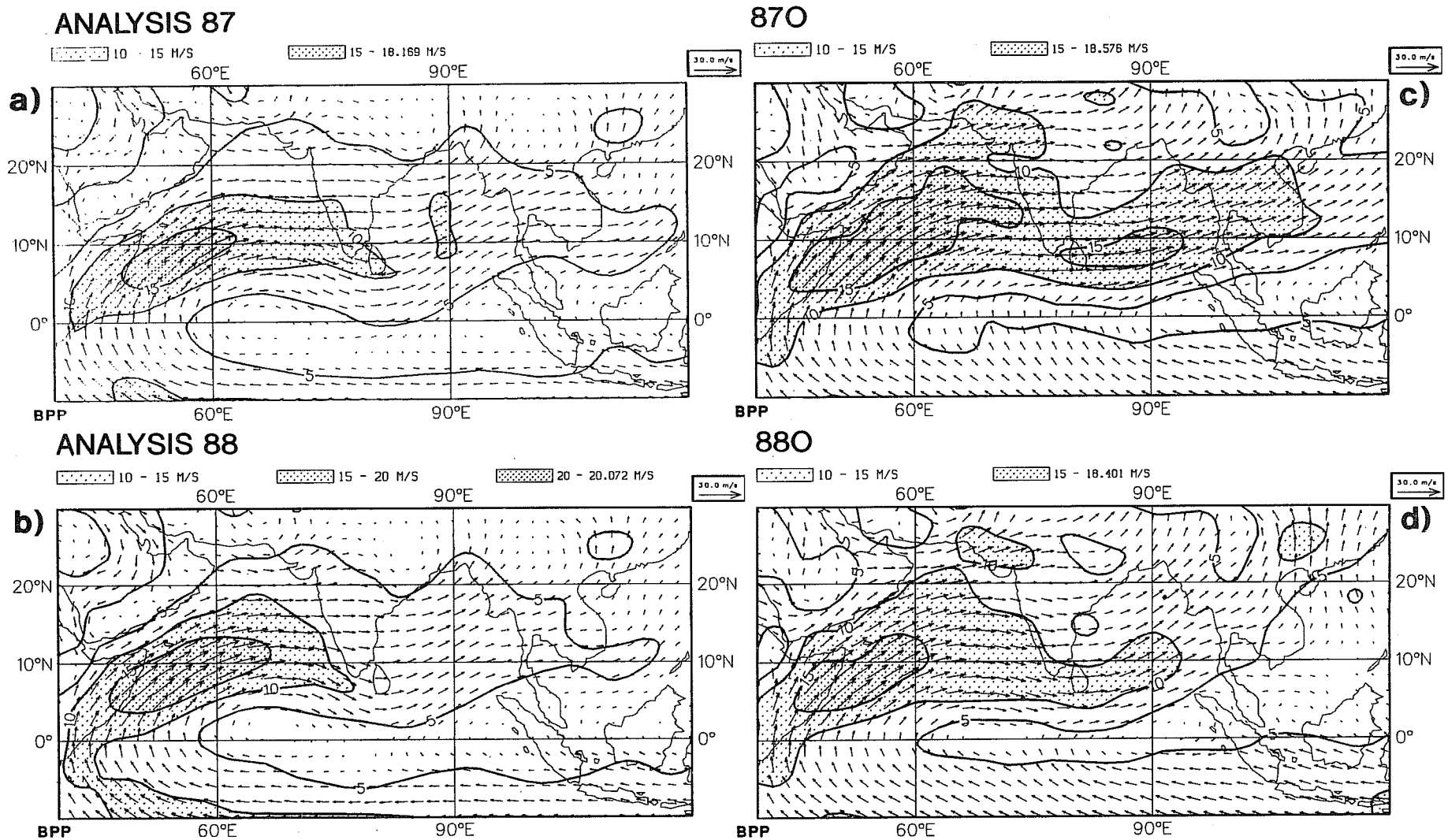

Fig. 11 850mb wind (m/s; June/July/August mean) Indian Ocean and surrounding regions. a) ECMWF analyses for 1987, b) ECMWF analyses for 1988, c) 87O, d) 88O. Stippled > 10 m/s.

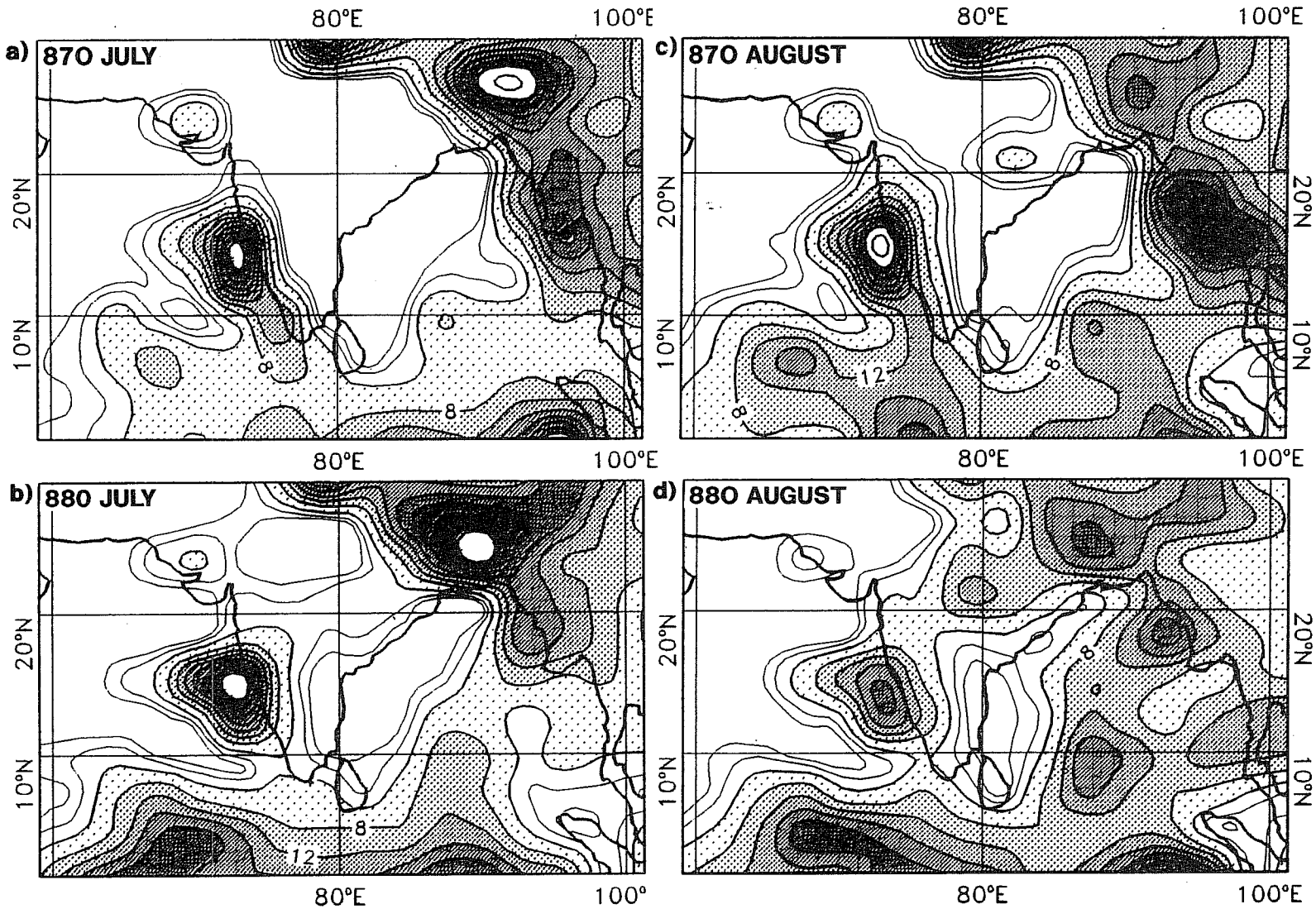

Fig. 12 Modelled rainfall over the Indian Subcontinent and surrounding areas of South Asia (mm/day) a) 87O July b) 88O July c) 87O August d) 88O August. Contours as Fig.9.

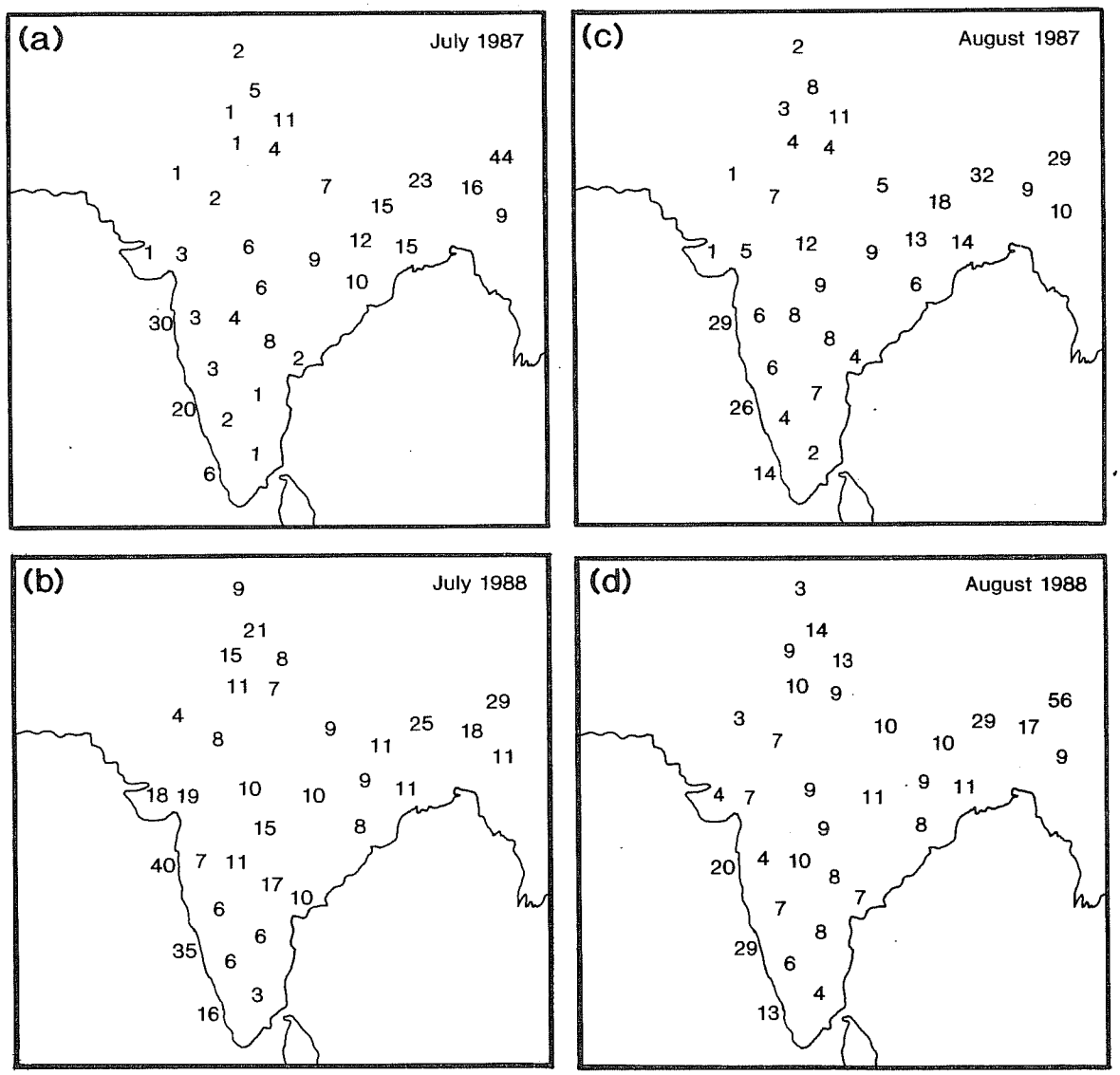

Fig.13. Observed rainfall over India (mm/day) based on subdivisional means (Das et al., 1988, 1989). a) July 1987 b) July 1988 c) August 1987 d) August 1988.

drought in July 1987 is manifest throughout India, with less rainfall in 1987 than 1988 in almost all the subdivisions. In this sense, the simulated rainfall differences between 87O and 88O are reasonable. However, it can be seen that, as in the Sahel, the simulated rainfall rates are considerably smaller than those observed, particularly in the Indian interior. For August, the difference in observed rainfall in the two years is less marked, though values in the Indian interior are still somewhat lower in 1987. Interestingly, rainfall in the west coast subdivisions are not significantly higher in 1988, and are noticeably lower for one subdivision. In this sense, the simulated rainfall differences between 87O and 88O are not unrealistic for August, though, as in July, absolute values are still too small.

For reference (see section c) we show in Fig.14, the mean rainfall difference for days 31-60, and 61-90 between 88O and 87O over Africa and south Asia. Note the consistent positive values over the Sahel and the south Indian Ocean. Differenes over India, while generally positive, are less consistent.

4.2 Influence of initial conditions

In the discussion above, comparing observed and simulated rainfall values, one might question the meaningfulness of a detailed comparison of values at the station or subdivisional level. In particular, if these values are not intrinsically predictable on these scales, such detailed comparison in not warranted. In section 3b, it was noted that the impact of interannual differences in SST, particularly over the Pacific, on seasonal-mean velocity potential and streamfunction , dominated the impact of initial conditions. To assess whether this conclusion still holds for local estimates of rainfall, we show in Fig.15a,b monthly mean rainfall differences for (88O-88O*), integrations with identical SST fields, but started one day apart.

Perhaps suprisingly in view of the earlier results, the monthly mean differences are by no means negligible. From Fig.15, these differences are smallest over the Sahel, and largest over the Indian Ocean. Indeed one might expect the Indian Ocean and west Pacific to be regions where local rainfall predictability is smallest, being areas where internal intra-seasonal variability is largest.

On the whole, the rainfall differences are not coherent from one month to the next (note, for example, the opposite rainfall differences over the Sahel, and the reversal of the sign of the maximum difference on the equator at about 65E.) However, the differences in Fig.15 a and b are not entirely cancelling, and indicate that whilst large-scale tropical velocity potential and streamfunction may be strongly predictable on the seasonal timescale, some aspects of regional month to seasonal tropical rainfall prediction are much less predictable.

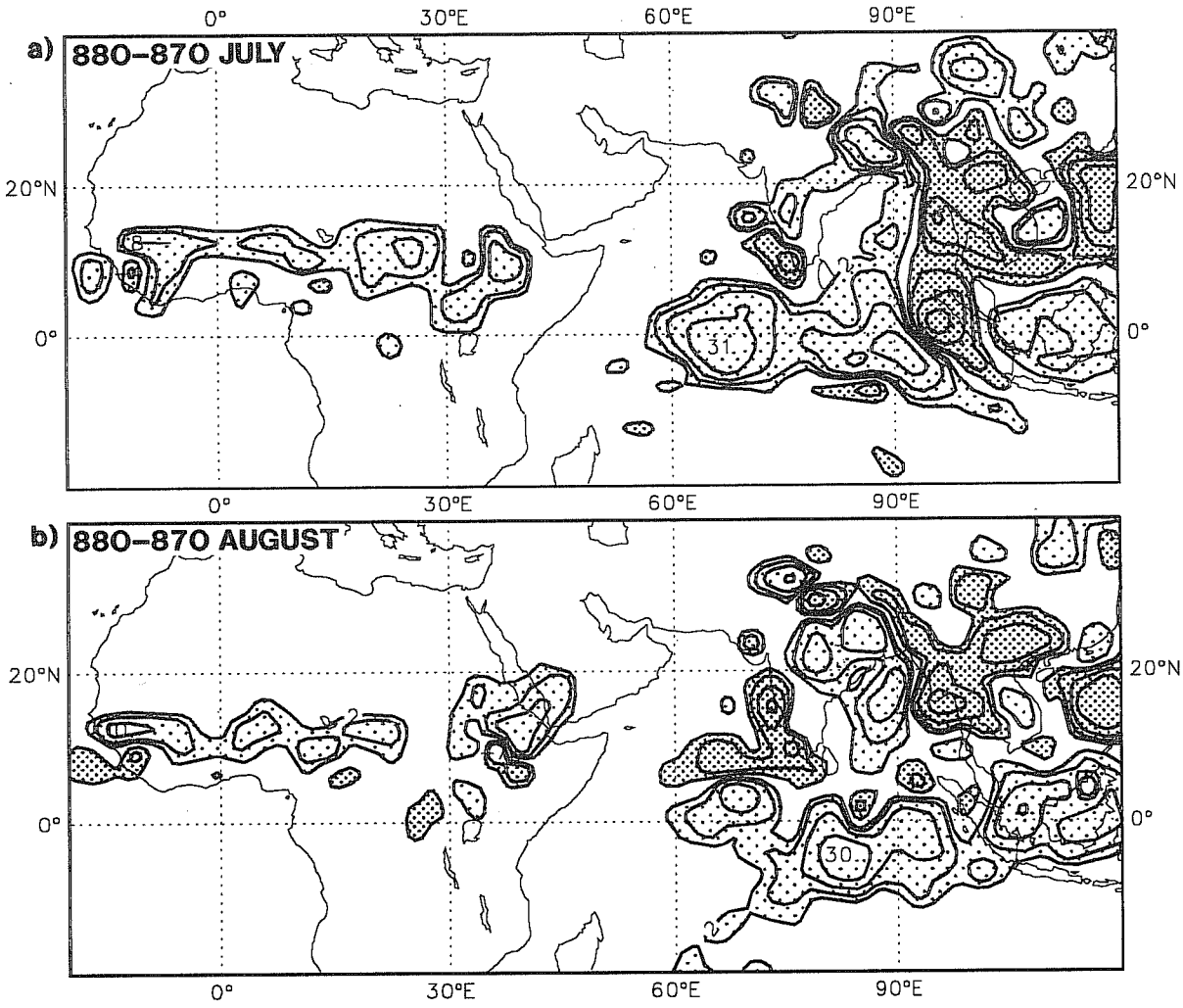

Fig.14. Rainfall differences averaged between a) days 31-60 b) days 61-90 for 88O-87O. Coarse stippling for values greater than 2mm/day, fine stippling for values less than -2mm/day. Contours at 2, 4, 8, 16 mm/day.

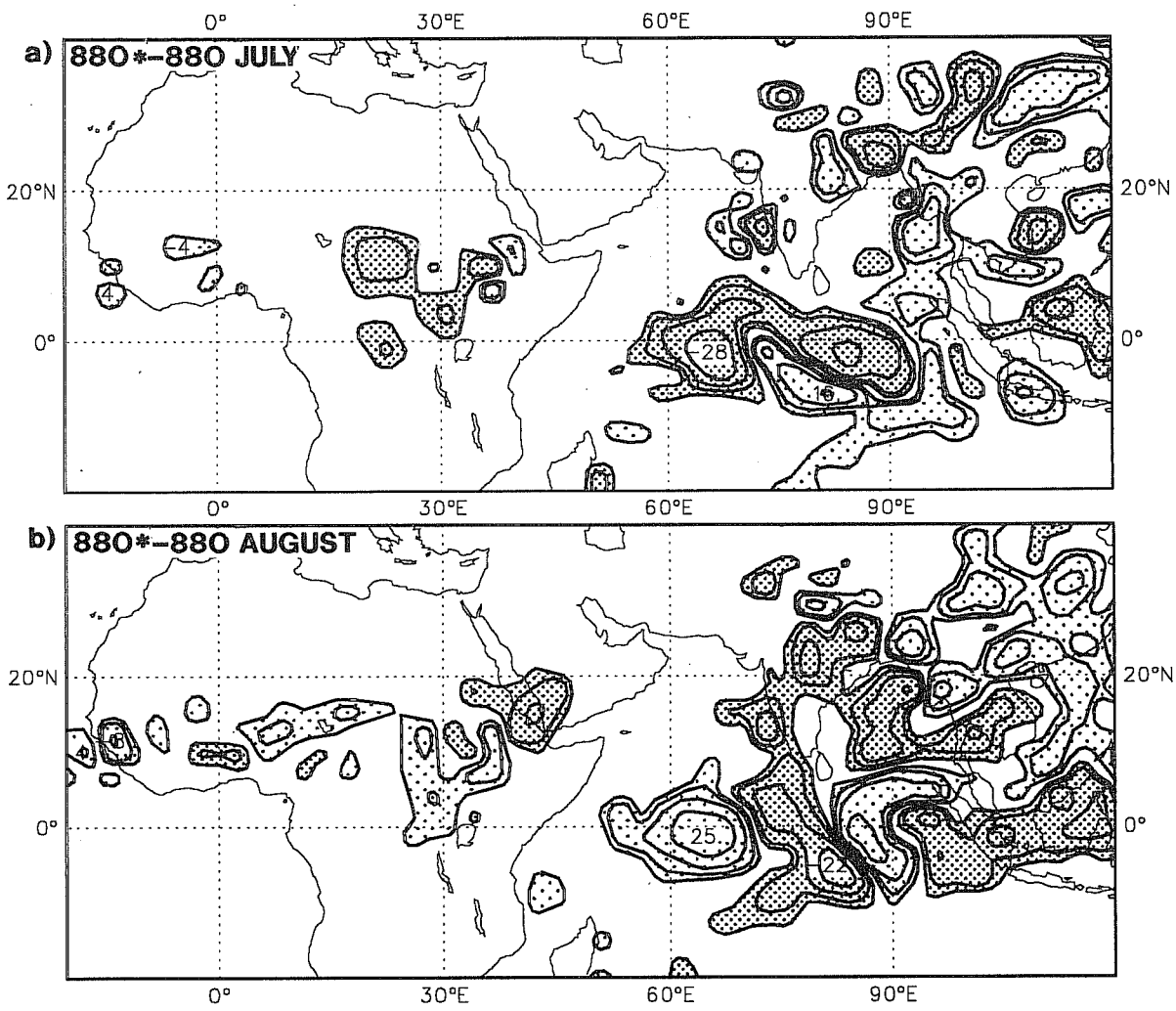

Fig.15. Rainfall differences averaged between a) days 31-60 b) days 61-90 for 88O*-88O. Stippling and contours as Fig.14.

From these results it appears that month to seasonal timescale rainfall is considerably more predictable over the Sahel than over India. This is consistent with the conclusions of Palmer et al. (1990) who studied 30-day mean rainfall predictions over a set of four years. Indeed, from the results shown in Fig.15, the predictability of month to seasonal rainfall for subdivisions of India may be limited. This aspect of the results clearly requires further study.

4.3 Integrations with regional SST anomalies

In Fig.16a-f, we show monthly-mean rainfall difference fields over Africa and South Asia between 'individual ocean' experiments (88OP-87OP), (88OI-87OI) and (88OA-87OA) respectively, for the last 60 days of the experiments. The SST difference field between the two years was shown in Fig.2, and the seasonal mean velocity potential and streamfunction differnece fields between these experiments was shown in Fig.7.

The 88OP-87OP differences (Fig.16 a,b) appear to induce a relatively large-scale impact on rainfall over this region, consistent (in sign) between the two months. Over most of the African Sahel, east Africa, India and the south Indian Ocean, rainfall is enhanced. On the other hand, there is some decrease in rain over the coastline of Burma. In many ways these differences are similar to those shown in Fig.14 for the full global observed SST fields.

For 88OI-87OI (Fig.16 c,d), the response is much more variable between the two months, despite large rainfall differences over the Indian Ocean in any one month. These fields are characteristic of the 'unpredictable' component in monthly mean rainfall discussed above. On this basis, it is not possible to conclude that interannual variability in Indian Ocean SST has a statistically significant impact on regional rainfall. Recently, Dube et al. (1990) have concluded that interannual variability of SST in the Arabian Sea is the passive response to variability in the monsoon system. Our results are consistent with these authors' findings.

For the tropical Atlantic Ocean anomalies (88OA-87OA; Fig.16e,f), the monthly-mean rainfall difference fields are also disimilar between the two months. As such we can conclude that the impact of interannual variability in Atlantic SST appers to be less important in accounting for interannual variations in Sahel rain than the impact of El Nino. At first sight this may seem inconsistent with earlier studies of the impact of SST on Sahel rainfall (e.g. Folland et al., 1986; Palmer, 1986), in which the importance of the Atlantic SST anomalies was emphasised. However, these studies were primarily focussed on the interdecadal variability of Sahel rainfall where coherent large-scale variability in Atlantic SST was evident.

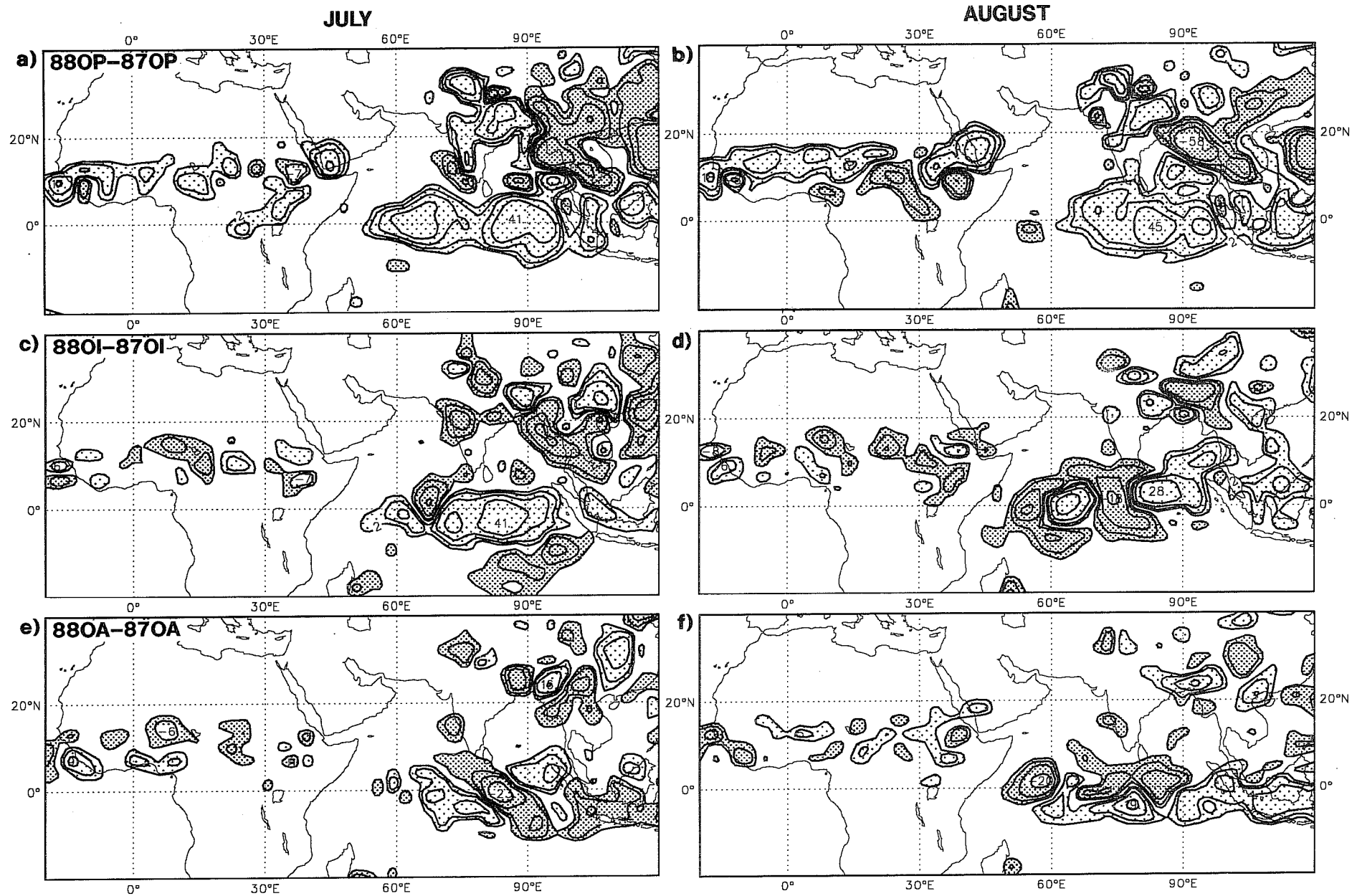

Fig. 16 Rainfall differences averaged between: 88OP-87OP a) 31-60 b) 61-90, 88OI-87OI c) 31-60 d) 61-90, 88OA-87OA e) 31-60 f) 61-90. Stippling and contours as Fig.14.

In view of the importance of resolving the question of whether Indian Ocean SST anomalies have a significant influence on rainfall in surrounding regions, we show in Fig.17a,b, rainfall differences, averaged over the last 60 days of the integrations, for 87OI-87C and 88OI-88C. As pointed out in the discussion above, the SST anomalies for these two years are indicative of interdecadel rather than interannual variability. As shown in Fig.6, the velocity potential difference fields indicated anomalous 200mb divergence over the Indian Ocean. The rainfall differences appear consistent with this, and show positive values on the equator between 60 and 70E. To the east, between 90 and 100E, there are consistent regions of negative rainfall differences. Note, however, that over India itself, there are no consistent differences between the two years.

5. CONCLUSIONS

A set of 90-day integrations has been made with a T42 version of the ECMWF operational model, from 1 June 1987 and 1 June 1988, forced with both observed and climatological sea surface temperature (SST) datasets. A brief description of the experiments was given in table 1. The following conclusions can be made.

With observed SSTs, the model was able to simulate with reasonable accuracy, the observed interannual variations in the global scale velocity potential and streamfunction fields, and in regional low-level monsoon flow on seasonal timescales. On the other hand, particularly for the integration for 1987, the model response tended to be larger that suggested by the analyses. Whilst this may indicate the need for further adjustment to some of the model's physical parametrizations, particularly with regard to surface flux formulation (cf Miller et al., 1991), it is likely that the analysed fields themselves underestimate the strength of the observed atmospheric anomalies.

When observed SSTs were used, simulated rainfall over the Sahel in 1987 was significantly weaker than in 1988 both in the second and third monthly mean periods (July and August). Simulated rainfall rates were verified using station data over the Sahel. These verifying values suggested that the model had an overall dry bias over the Sahel. Similar conclusions were found for the Indian subcontinent, though overall the agreement between simulations and observations was less good. A similar dry bias was found for Indian rainfall.

The sensitivity of the simulations to initial conditions was studied by running an additional integration for 1988 from 2 June. Whilst the simulation of large-scale seasonal-mean velocity potential and streamfunction in the tropics was relatively insensitive to atmospheric initial conditions compared with the impact of the imposed SST anomalies, month to seasonal regional rainfall was sensitive to initial conditions, particularly over the east Indian ocean, south east Asia, and the west Pacific. Further to

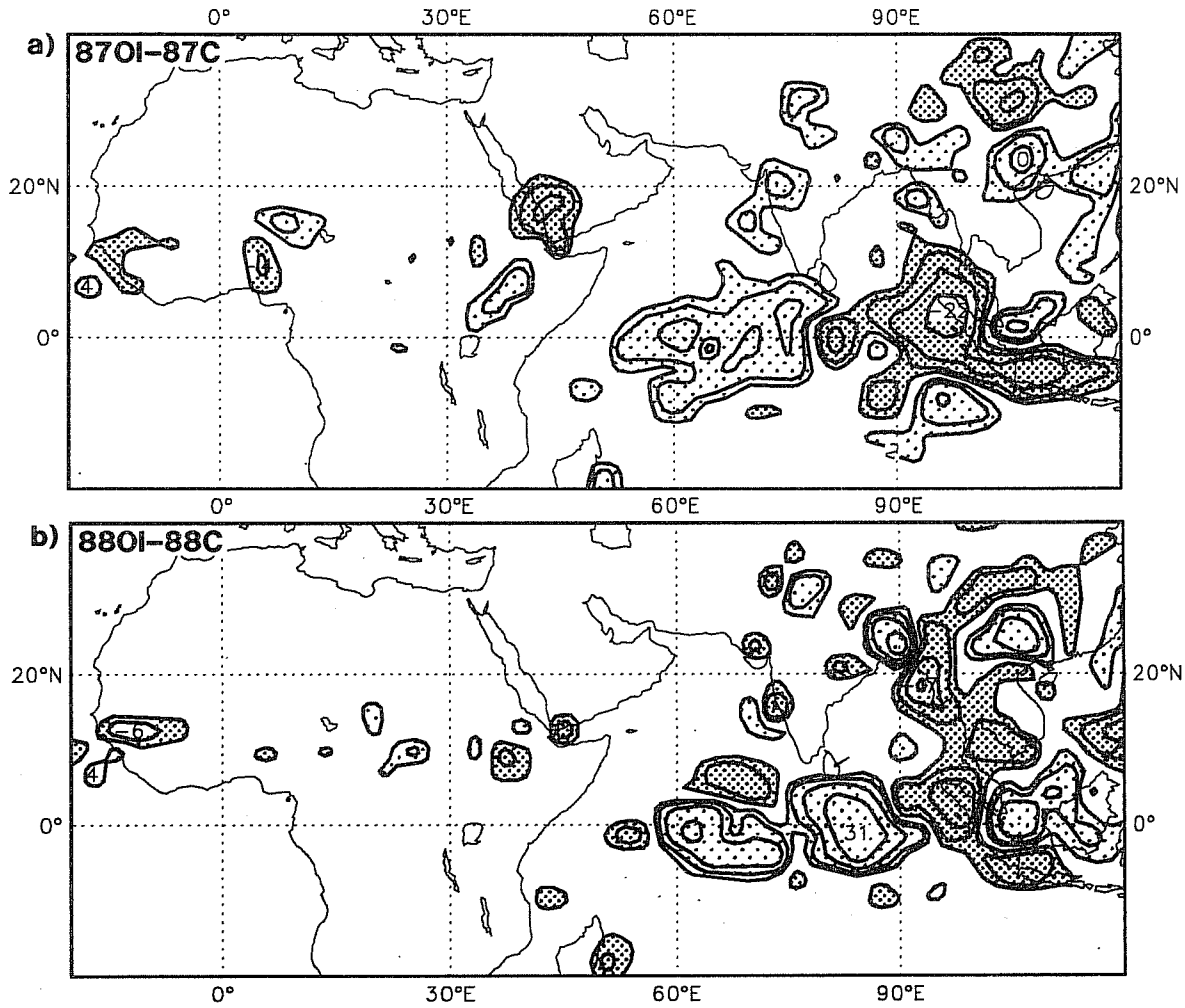

Fig.17. Rainfall differences averaged between days 31-90 for a) 87OI-87C b) 88OI-88C. Stippling and contours as Fig.14.

the west, e.g. over the African Sahel, regional rainfall was less sensitive to initial conditions. India itself lies somewhat at the boundary between these two regions, and results indicate that intrinsic predictability of month to seasonal rainfall over India at the subdivisional scale may be somewhat limited.

The impact of SST anomalies in the individual oceans was studied. Interannual differences in rainfall over the Sahel and India between 1987 and 1988 were associated almost entirely with the remote effect of the tropical Pacific SST anomalies. The Indian Ocean, somewhat cooler in 1988 than in 1987, did not appear to have a significant impact on the simulated monsoon rains. Moreover, whilst the Indian Ocean was found to be warm relative to climatology in both 1987 and 1988, and whilst the impact of these anomalies produced a consistent increase in rain in the model over the Indian Ocean, the impact of these Indian Ocean SST anomalies on rainfall over Indian itself, was not significant. Overall these results are supported by observational studies suggesting that Indian monsoon rainfall is correlated more strongly with Pacific SST anomalies, than with Indian Ocean SST anomalies (Shukla and Paolino, 1983).

These integrations have been made with the complete ECMWF land/surface parametrizations, and variation in land surface variables (e.g. soil moisture) between the two initial datasets are included. In this study we have deliberately chosed to focus on the impact of SST itself. However, this does not imply that these initial land surface differences are unimportant in accounting for the either the observed or simulated differences in monsoon rains. Indeed, comparison of two runs with identical SSTs, but land surface (and atmospheric) initial conditions one year apart, suggest that the Sahel rain in particular may be significantly influenced by land surface conditions.

Studies such as these would benefit from consistent SST and atmospheric climatological datasets, and lend support to the requirement for atmospheric reanalysis (Bengtsson and Shukla, 1988). Moreover, the results of this study justifies more extensive experimentation with a higher resolution version of the model. A more extensive investigation of the predictability of month to seasonal rainfall over regions of the tropics appear to be warranted.

REFERENCES

Bengtsson, L. and J. Shukla, 1988: Integration of space and in situ observations to study global climate change. Bull.Amer.Meteor.Soc., 69, 1130-1143.

Charney, J.G. and J.Shukla, 1981: Predictability of monsoons. In: Monsoon Dynamics, Eds J.Lighthill and R.Pearce. Cambridge University Press, 735pp.

Das, S.N., M.R.M. Rao and N.C. Biswas, 1988: Monsoon season (June-September 1987). Mausam, 39, 325-340.

Das, S.N., D.S.Desai and N.C. Biswas, 1989: Monsoon season (June-September 1988). Mausam, 40, 351-364.

Dube, S.K., M.E. Luther and J.J. O'Brien, 1990: Relationships between interannual variability in the Arabian Sea and Indian Summer Monsoon. Meteor.Atmos.Phys., 44, 153-165.

Folland, C.K., D.E. Parker and F.E. Kates, 1984: Worldwide marine temperature fluctuations 1856-1981. Nature, 310, 670-673.

Folland, C.K., T.N. Palmer and D.E. Parker, 1986: Sahel rainfall and worldwide sea temperatures. Nature, 320, 602-607.

Folland, C.K., J.A. Owen and K. Maskall, 1989: Physical causes and predictability of variations in seasonal rainfall over sub-Saharan Africa. IAHS Publ. No.186, 87-95.

Gill, A.E., 1980: Some simple silutions for heat-induced tropical circulations. Q.J.R. Meteor.Soc., 106, 447-462.

Krishnamurti, T.N., H.S. Bedi and M. Subramaniam, 1989: The summer monsoon of 1987. J.Climate, 2, 321-340.

Krishnamurti, T.N., H.S. Bedi and M. Subramaniam, 1990: The summer monsoon of 1988. Meteorol. Atmos. Phys., 42, 19-37.

Lamb, P.J., 1983: West African water vapor variations between recent contrasting Subsaharan rainy seasons. Tellus, 35A, 198-212.

Miller, M.J., Beljaars, A. and T.N.Palmer, 1991: The sensitivity of the ECMWF model to the parametrization of evaporation from the tropical oceans. J.Clim. *Submitted.*

Palmer, T.N., 1986: Influence of the Atlantic, Pacific and Indian Oceans on Sahel rainfall. Nature, 322, 251-253.

Palmer, T.N., C.Brankovic, F.Molteni and S.Tibaldi, 1990: Extended-range predictions with ECMWF models: Interannual variability in operational model integrations. Q.J.R. Meteor.Soc., 116, 799-834.

Reynolds, R.W. and L. Roberts, 1987: A global sea surface temperature climatology from in situ, satellite and ice data. Trop. Ocean-Atmos. Newsletter, 37, 15-17.

Reynolds, R.W., 1988: A real-time global sea surface temperature analysis. J.Clim., 1, 75-86.

Shukla, J., 1987: Interannual variability of monsoons. In: Fein, J.S., Stephens, P.L. (Eds) Monsoons. New York: Wiley, 632pp.

Shukla, J., and D.A. Paolino, 1983: The Southern Oscillation and long-range forecasting of the summer monsoon over India. Mon.Wea.Rev., 111, 1830-1837.

Simmons, A.J., Burridge, D.M., Jarraud, M., Girard, C. and Wergen, W., 1988: The ECMWF medium-range prediction models: Development of the numerical formulations and the impact of increased resolution. Meteor.Atmos.Phys., 40, 28-60.

WMO, 1986: Workshop on comparison of simulations by numerical models of the sensitivity of the atmospheric circulation to sea surface temperature anomalies. WMO/TD-No 138, WCP-121, 188pp.

WMO, 1988: Modelling the sensitivity and variations of the Ocean-Atmosphere system. WMO/TD-No 254, WCRP-15, 289pp.